JOINT INSTITUTE FOR NUCLEAR RESEARCH
Flerov laboratory of Nuclear Reactions

FINAL REPORT ON THE START PROGRAMME

Differential cross section reaction products of ^{7}Li + ^{10}B interaction

Supervisor:
Dr. Yuri Gennadievich Sobolev

Student:
Tran Hai Phong, Viet Nam
VNU - University of Science

Participation period:
September 07 – October 19,
Summer Session 2025

Dubna, 2025

Abstract

The differential cross-sections of $^{7}Li_{g.s.}$, $^{6}Li_{g.s.}$, $^{6}Li^{*}_{3.56}$, $^{6}He_{g.s.}$ and $^{7}Be_{g.s.}$ reaction products emitted from the $^{7}Li+^{10}B$ collision are measured in the angular range ($11^{0} < \theta_{CM} < 84^{0}$) in a single experiment under the same conditions.

The experiment was carried out using a ^{7}Li beam at E_{LAB} = 58 MeV of U-400 cyclotron, FLNR JINR, Dubna.

These measurements provide essential experimental data for further investigation of nucleon transfer processes and structural features of light nuclear systems. Of particular interest of our studies are:

1) The spatial properties of the $^{6}Li^{*}_{3.56}$ nuclear state since it is an isobar-analogue state $^{6}He_{g.s.}$ exotic nucleus, which has a 2*n*-halo structure.
2) Properties ^{7}Be nucleus, which is a mirror nucleus of ^{7}Li and is formed in $^{10}B(^{7}Li, ^{7}Be)^{10}Be$ charge exchange reaction.

The results serve as a basis for subsequent theoretical interpretation and modeling of cluster and halo phenomena in Li and Be isotopes.

I. Introduction

Light nuclei occupy a central position in nuclear physics research due to their relatively simple structure and the pronounced quantum effects that govern their behavior. These systems, including isotopes of helium, lithium, boron, and beryllium, serve as ideal platforms for investigating fundamental nuclear properties such as nucleon transfer dynamics, cluster configurations, and halo phenomena. Their low mass numbers and reduced complexity make them particularly suitable for testing theoretical models and exploring the interplay between single-particle motion and collective nuclear behavior.

Beyond their relevance to nuclear structure studies, light nuclei play a vital role in astrophysical processes, especially in stellar nucleosynthesis. Reactions involving light ions contribute to the formation of elements in stars and are essential for understanding the evolution of matter in the universe. As such, experimental investigations of light-ion induced reactions not only advance nuclear theory but also provide valuable data for astrophysical modeling.

Among the various reaction mechanisms, charge exchange reactions and nucleon transfer processes are of particular interest. Charge exchange reactions, which involve the exchange of a proton for a neutron or vice versa, allow access to isobaric analog states and offer insight into spin-isospin excitations. These reactions are sensitive to the internal structure of the nucleus and can reveal subtle features such as neutron skin thickness and isospin symmetry breaking. When applied to light nuclear systems, they help elucidate the formation of exotic configurations, including cluster states and halo structures near the drip lines.

In recent years, growing attention has been directed toward the spatial properties of light nuclei, especially those exhibiting halo-like behavior in their ground or excited states. For instance, the isotope ^{6}Li has been the subject of extensive theoretical and experimental scrutiny due to inconsistencies in its

measured root-mean-square (rms) radius, which ranges from 2.09 ± 0.02 fm [1] to 2.54 ± 0.10 fm [2]. These discrepancies highlight the need for more precise measurements to clarify its internal structure. Furthermore, theoretical models such as the No-Core Shell Model (NCSM) [3] suggest that excited states of ^{6}Li, particularly the 3.56 MeV state, may exhibit extended spatial configurations comparable to halo structures observed in ^{6}He.

Experimental studies of the energy dependence of the total cross sections $\sigma_R(E)$ for the ^{6}Li+^{28}Si reactions [4] showed that in the beam energy range E_{LAB}~10-20 MeV/nucleon the cross section has a local maximum (bump), similar to $\sigma_R(E)$ that previously discovered in the ^{6}He+^{28}Si reaction [5], see Fig.1.

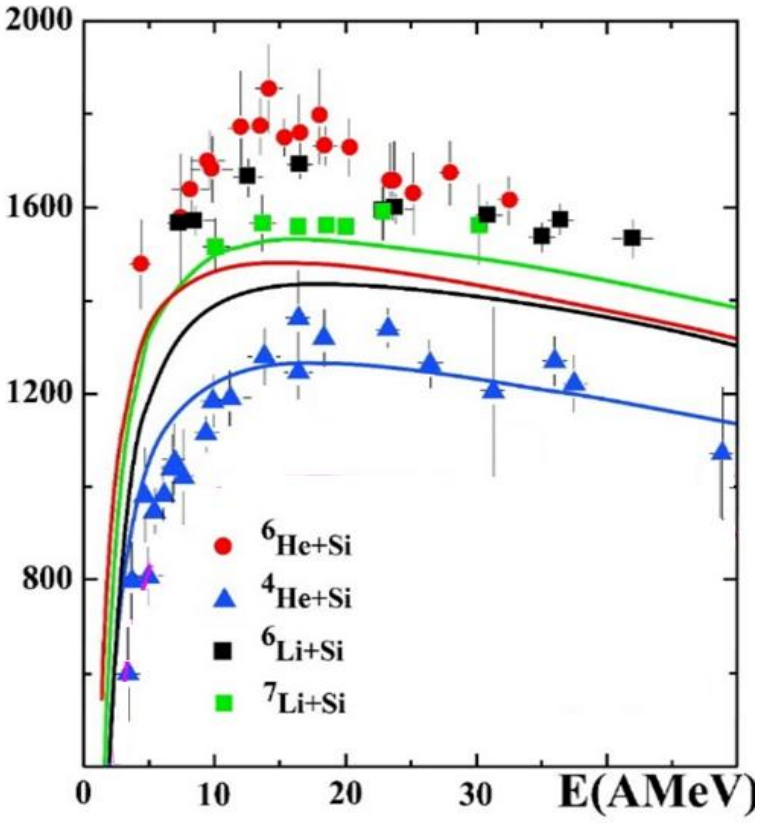

Fig.1. Experimental total cross sections for the reactions: ^{4}He+^{28}Si (blue triangles) [5], ^{6}He+^{28}Si (red circles) [5], ^{6}Li+^{28}Si (black squares) [4] and ^{7}Li+^{28}Si (green squares) [5] in comparison with the empirical Kox parametrization formulas in [14–16] (curves of the corresponding color).

As is clearly seen from Fig.1, the values of $\sigma_R(^{6}\text{He},^{6}\text{Li}+^{28}\text{Si})$ exceed the values of $\sigma_R(^{7}\text{Li}+^{28}\text{Si})$ at E_{LAB} = (7-20) AMeV. Thus, an additional argument for

studying the spatial properties of $^{6}Li_{g.s.}$ lies in the peculiarities of the $\sigma_R(E)$ $^{6}He,^{6}Li+^{28}Si$ reactions at E_{LAB} = (7—20) AMeV [4, 5].

The ^{6}Li nucleus is the least deformed of the region of light nuclei (see Fig. 2 from [6]), therefore the local enhancement of $\sigma_R(E)$ reaction $^{6}Li+^{28}Si$ at E_{LAB} = (7-20) AMeV cannot be explained by ^{6}Li deformation.

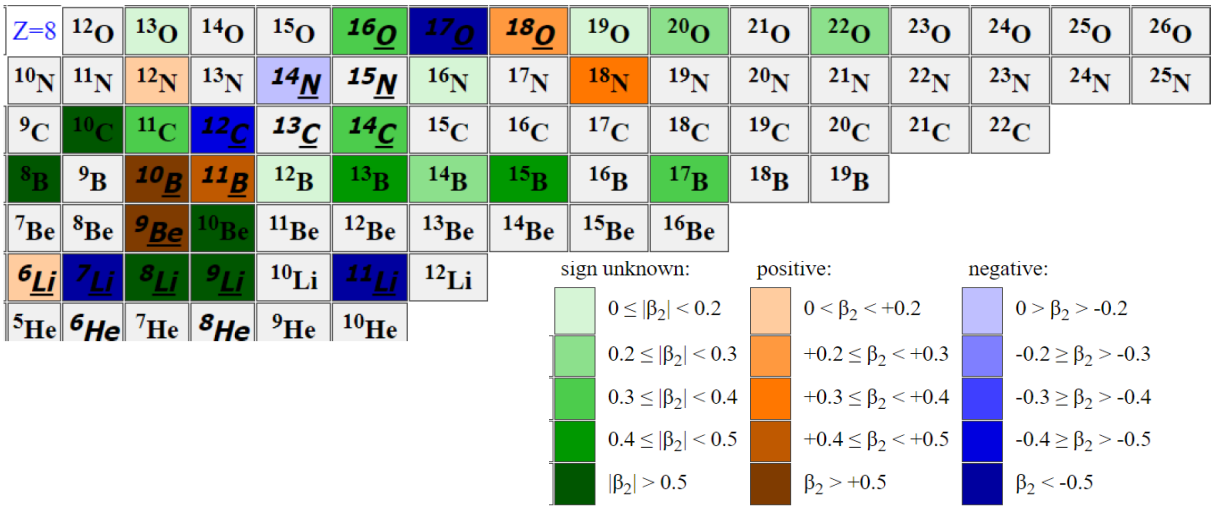

Fig.2. The landscape of β_2 quadrupole deformation of light nuclei region from [6] http://cdfe.sinp.msu.ru/services/radchart/radmain.html.

One of the issues in the study of exotic nuclei is the question of preserving the properties of the halo in excited isobaric analogue states, since due to the isospin symmetry of the strong interaction, the state $^{6}Li^{*}(0^{+}, T=1, E=3.56$ MeV) should have similar spatial and spin characteristics of the wave function, the same as the ground state of ^{6}He.

The most accessible experiments for this are those with beams of stable ^{6}Li nuclei included in the isobaric triplet A=6 (^{6}He-^{6}Li-^{6}Be), see Fig.3.

Among these triplet states, the neutron halo in ^{6}He is well known. A *p*-*n* halo is predicted in the excited state $^{6}Li(0^{+}$, 3.56 MeV) in which lies only 137 keV below the value of $^{6}Li \rightarrow ^{4}He+p+n$ reaction threshold. Its radius is not known, but it is predicted by about 0.25 Fm larger than the radius of ^{6}He [7,8].

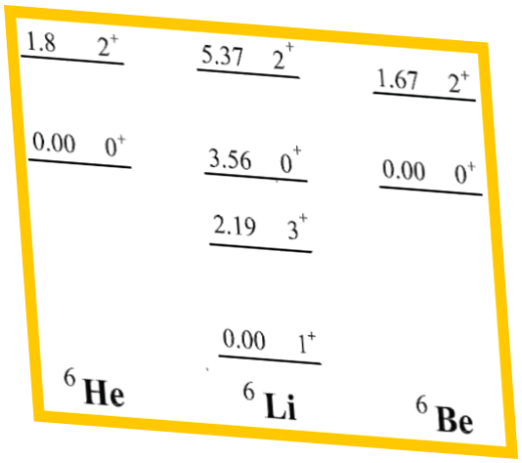

Fig.3. The states of the triplet ^{6}He-^{6}Li-^{6}Be are presented. of ^{6}He(0^{+}, 0.0 MeV), ^{6}Li(0^{+}, 3.56 MeV) and ^{6}Be(0^{+}, 0.0 MeV) are isobar-analogues.

So, the experimental data on the spatial structure of excited state ^{6}Li(0^{+}, 3.56 MeV) which is IAS of ^{6}He(0^{+}, 0.0 MeV) halo state are significantly limited.

These IAS states, especially ^{6}Li(0^{+}, 3.56 MeV), are best explored using direct reaction channels such as stripping or pick-up of single-nucleon which provide cleaner access to specific nuclear states and reduce the complexity associated with multi-step processes.

Properties ^{7}Be nucleus, which is a mirror nucleus of ^{7}Li and is formed in ^{10}B(^{7}Li, ^{7}Be)^{10}Be charge exchange reaction.

In the past decade, light mirror nuclei—isobaric pairs where the number of protons in one nucleus equals the number of neutrons in the other—have attracted considerable research interest. These pairs offer powerful tools for studying nuclear structure and isospin symmetry.

In the idealized scenario of exact isospin symmetry, originally proposed by Heisenberg, protons and neutrons differ only in charge, resulting in identical energy spectra in mirror nuclei, with the exception of a constant Coulomb shift.

Recent research in this area has focused on pairs of mirror nuclei, such as (^{9}Be - ^{9}B), (^{10}Be - ^{10}C), and (^{11}B - ^{11}C), produced in the ^{10}B + ^{10}B reaction [9].

From this perspective, it is of interest to study the isobaric pair (^{7}Li - ^{7}Be) of mirror nuclei which is produced in the charge-exchange ^{10}B(^{7}Li, ^{7}Be)^{10}Be reaction.

In this context, the interaction between ^{7}Li and ^{10}B at an incident energy of 58 MeV presents a rich opportunity to study reaction channels leading to helium, lithium and beryllium isotopes. These isotopes are known to exhibit complex structural behavior, and their formation through transfer reactions provides a window into the underlying nuclear dynamics. Measuring the angular distributions of differential cross sections for these channels is a crucial step in identifying dominant reaction mechanisms and extracting information about the residual nuclei.

The present work focuses on the experimental determination of angular distributions of reaction products from the ^{7}Li+^{10}B interaction. The measurements were carried out using the U-400 cyclotron at the Flerov Laboratory of Nuclear Reactions (FLNR), JINR Dubna. The collected data serve as a foundation for further theoretical analysis and modeling, contributing to a deeper understanding of nucleon transfer processes and structural phenomena in light nuclear systems.

II. Experimental setup

In this study, angular distributions of differential cross sections for the ^{7}Li+^{10}B reaction were measured using the U-400 cyclotron at the Laboratory of Nuclear Reactions, JINR Dubna. A schematic layout of the experimental setup is shown in Fig. 4. The ^{7}Li beam, accelerated to 58 MeV with an energy resolution of ΔE (FWHM) = 0.5 MeV, was guided and focused through a magnetic system and a position-sensitive multiwire “X-Y” chamber. Beam shaping was achieved using diaphragms D1–D4, forming a collimator at the target position M. The resulting beam spot had a Ø = 3.6 mm and an angular spread of $\Delta\theta \approx 0.2°$.

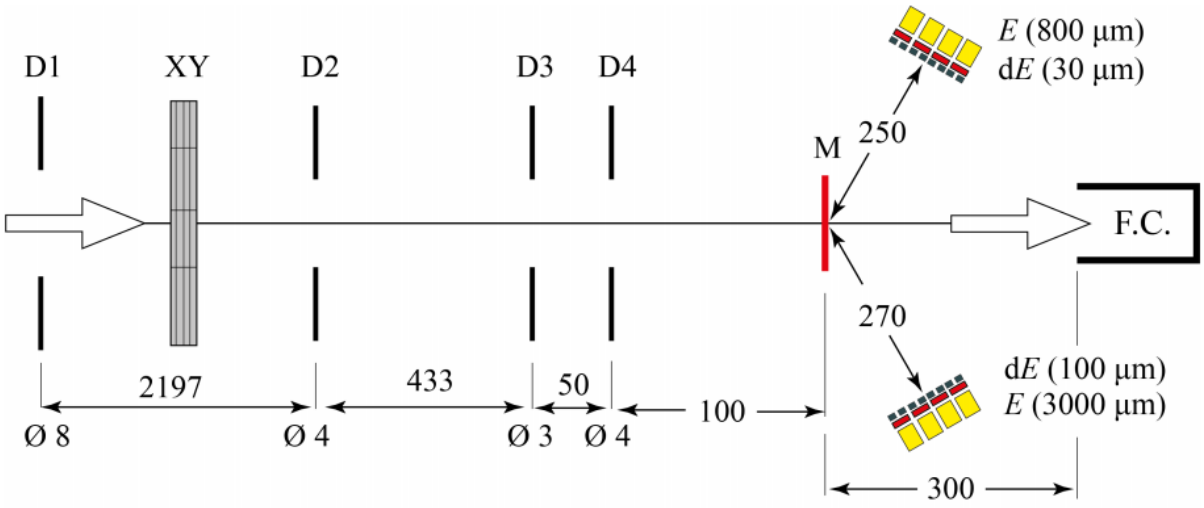

Fig. 4: Experimental scheme for angular distribution measurements in the ^{7}Li+^{10}B reaction.

The target consisted of a self-supporting ^{10}B foil (thickness $H \approx 0.05$ mg/cm², diameter Ø ≈ 1.0 cm), mounted perpendicular to the beam axis. Isotopic impurities of ^{12}C (9%) and ^{16}O (6%) were present and estimated using known elastic scattering data from similar reactions at nearby energies (E_{LAB} = 36 MeV and 39 MeV).

A Faraday cup, located 30 cm downstream from the target, was used to monitor beam current. It consisted of a steel cylinder (diameter Ø = 4 cm, height 25 cm, wall thickness $H \approx 0.5$ cm). Beam current data were recorded via an ORTEC–439 integrator and synchronized with event data using a dedicated DAQ system.

Beam and target conditions were additionally monitored using a Si(Li) detector (not shown in Fig. 4).

The DAQ system included VME modules (MVLC crate controller, MADC-32 ADC) and NIM logic units, operated via the Mesytec MVME software. The MVLC module served as the master trigger, receiving signals from detectors and the beam integrator. DAQ dead time was evaluated by comparing trigger requests and recorded events.

Fig.5. A photo of the reaction chamber (top view)

Two detector groups were deployed to measure reaction products. Each group consisted of four Δ*E*–*E* telescopes. The first group, covering forward angles (7° < θ < 30°), included two pairs of telescopes, each with two Δ*E* detectors (100 μm thick, 12×12 mm² sensitive area) and one *E* Si(Li) detector (3000 μm thick, 20 mm diameter). The second group, positioned at angles θ > 17°, used telescopes with a 30 μm Δ*E* detector (20 mm diameter) and an 800 μm strip *E* detector (6×50 mm² per strip).

The θ_{LAB} -angular position of each group of Δ*E*–*E* telescopes was changed independently with an accuracy of $\Delta\theta = 0.1^0$ and without breaking the vacuum in the reaction chamber (See Fig.5.). A photo of the reaction chamber (top view) is shown in Fig. 5.

Lead collimators (~3×4 mm²) were placed in front of each telescope, defining solid angles of $\Omega = 1.3\times10^{-4}$ sr and 2.2×10^{-4} sr for the first and second groups, respectively. Angular spacing between adjacent telescopes was θ_{LAB}= 3.2° and 1.7°, with angular precision of ± 0.5°. Energy resolution of the Δ*E* and *E* detectors was better than 60 keV, verified using a ^{226}Ra α-source.

III. Results and Analysis

3.1 Based on the experimental spectrum analysis method

Conducting the experiment with a ΔE–E telescope system yields a two-dimensional $\Delta E \times E$ spectrum, as shown in Fig. 6, which reflects the ionization energy losses of the reaction products from ^{7}Li+^{10}B at an angle θ_{Lab}=22.3°, using silicon detectors with thicknesses of 30 μm for the ΔE layer and 700 μm for the E layer. In this detection system, charged particles lose energy as they pass through both detector layers, with the amount of energy loss depending on their mass and charge. This process produces distinct curved tracks in the $\Delta E \times E$ plane, which represent particle type.

The amount of energy lost in each layer depends on the particle's physical properties such as mass, charge, and initial energy. This energy loss process follows the stopping power law, described by the Bethe-Bloch formula, where the rate of energy loss is proportional to the square of the particle's charge and inversely proportional to the square of its velocity. Light particles such as protons, deuterons, or tritons will follow different paths in the $\Delta E \times (E+\Delta E)$ plane compared to heavier particles like α, ^{6}Li, or ^{7}Li.

However, in practice, the experimental spectrum is often affected by background noise, limited energy resolution, and overlapping reaction channels. Especially when multiple particle types are present, visual identification becomes challenging. Therefore, accurate particle identification requires theoretical modeling and simulation support.

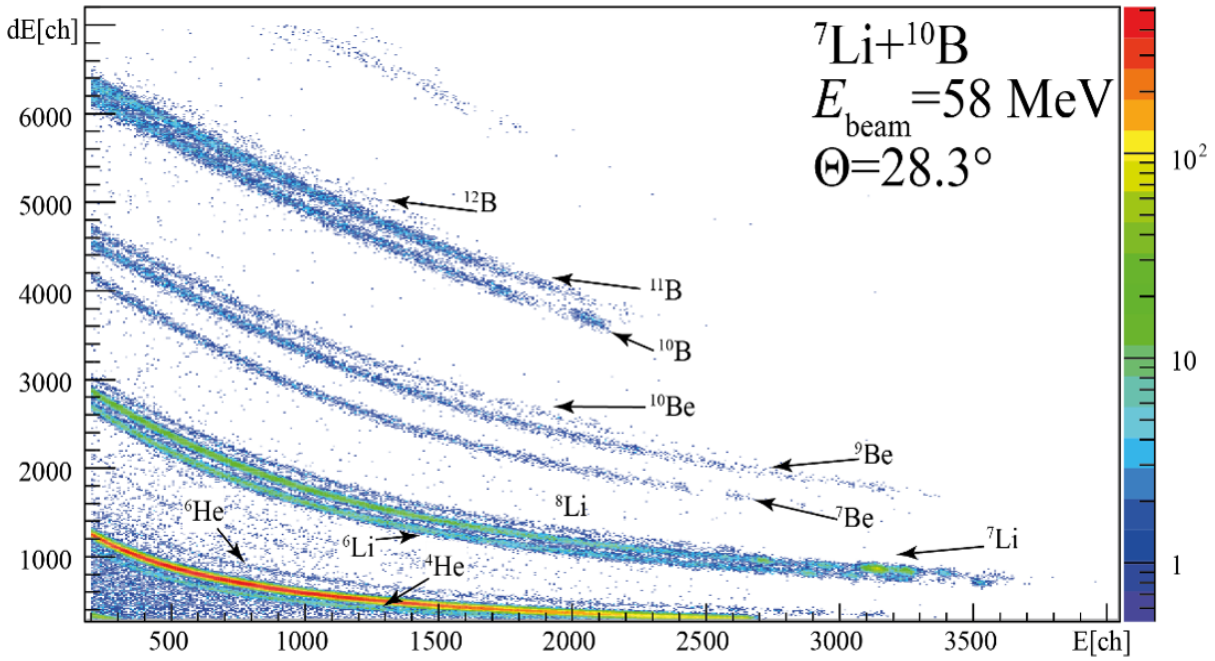

Fig. 6: Two-dimensional $\Delta E \times (E+\Delta E)$ spectrum of the reaction products from the ^{7}Li+^{10}B reaction, recorded using a ΔE–E telescope at a laboratory angle of $\theta_{Lab} = 22.3°$ with a beam energy of $E_{BEAM} = 58$ MeV.

LISE^{++} [10] software was developed to assist in this process. It is a powerful tool that simulates the energy loss of particles passing through detector layers, based on both empirical models and theoretical frameworks describing charged particle interactions with matter. Users can configure parameters such as particle type, incident energy, detector material, and layer thickness. The software then calculates the energy loss in each layer and outputs corresponding ΔE and E data.

The simulation is performed by scanning the incident energy over a defined range (e.g., from 10 MeV to 50 MeV). For each energy value, the software computes the energy lost in the ΔE layer and the remaining energy deposited in the E layer, generating a set of $\Delta E \times E$ points for each particle. This set forms the theoretical curve of that particle in the $\Delta E \times E$ spectrum. Repeating this procedure for various particles such as protons, deuterons, tritons, α, ^{6}Li, and ^{7}Li produces a collection of theoretical contours (Fig. 7).

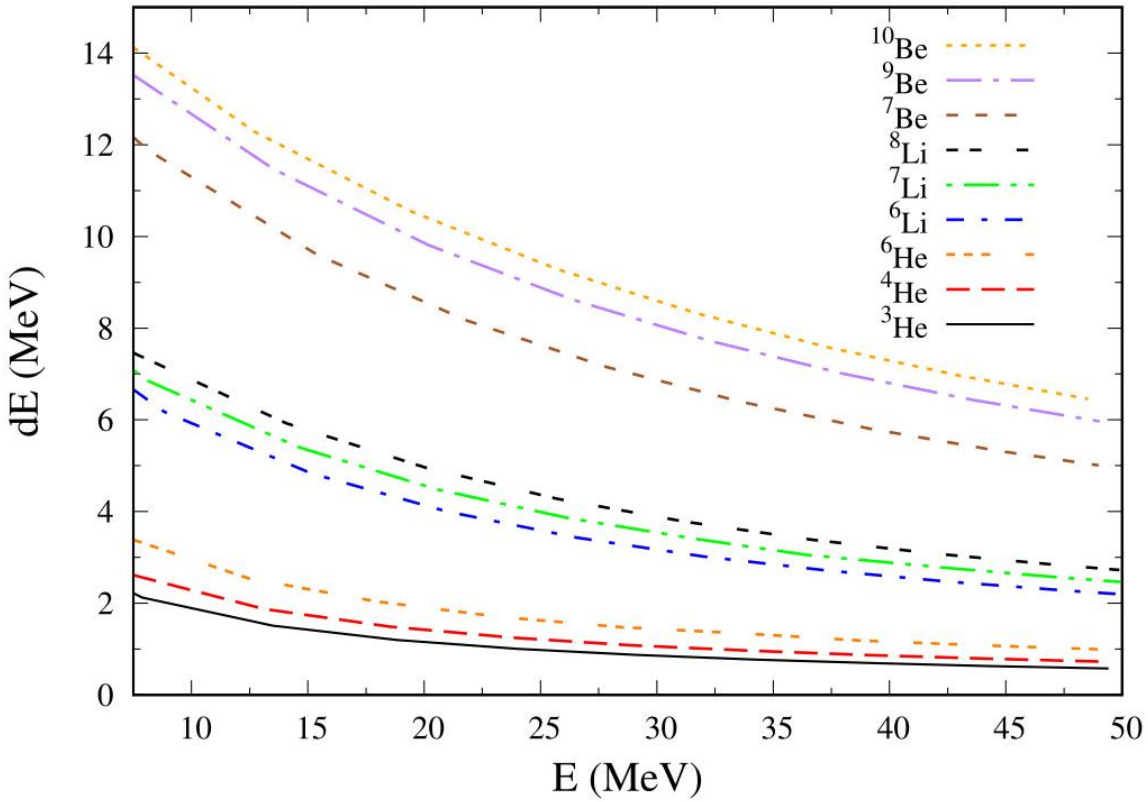

Fig. 7: Simulated two-dimensional energy spectrum of isotopes ^{3}He-^{10}Be in the *dE* – *E* telescope detectors caculated using the LISE^{++} package [10].

These curves are overlaid onto the experimental spectrum for comparison, enabling precise identification of the particle types associated with each band. Additionally, LISE^{++} allows users to incorporate the energy resolution of the beam and detector system, thereby simulating realistic contour shapes. This is especially useful for defining gating regions, eliminating background noise, and separating different reaction channels.

To construct one-dimensional spectra from the two-dimensional data shown in Fig. 6, we apply contour-based integration techniques for particle identification. Fig. 6 displays a particle identification map using the combination of energy loss (*dE*) and total energy (*E*), where each curved band corresponds to a distinct isotope such as ^{6}Li, ^{7}Be, ^{10}B, and others. By accurately defining contour regions around each band, we can isolate events associated with specific particles.

Once the contour for a given isotope (e.g., ^{6}Li$_{g.s.}$) is selected, the counts are integrated along the energy axis to generate a one-dimensional spectrum, as shown in Fig. 8. This spectrum plots the number of counts (*N*) versus energy

(*E*), allowing identification of nuclear states through peak positions and shapes. Building one-dimensional spectra from two-dimensional contour maps not only reduces background noise but also enhances the precision of reaction channel analysis, enabling extraction of cross sections, excitation energies, and nuclear structure information for the reaction products.

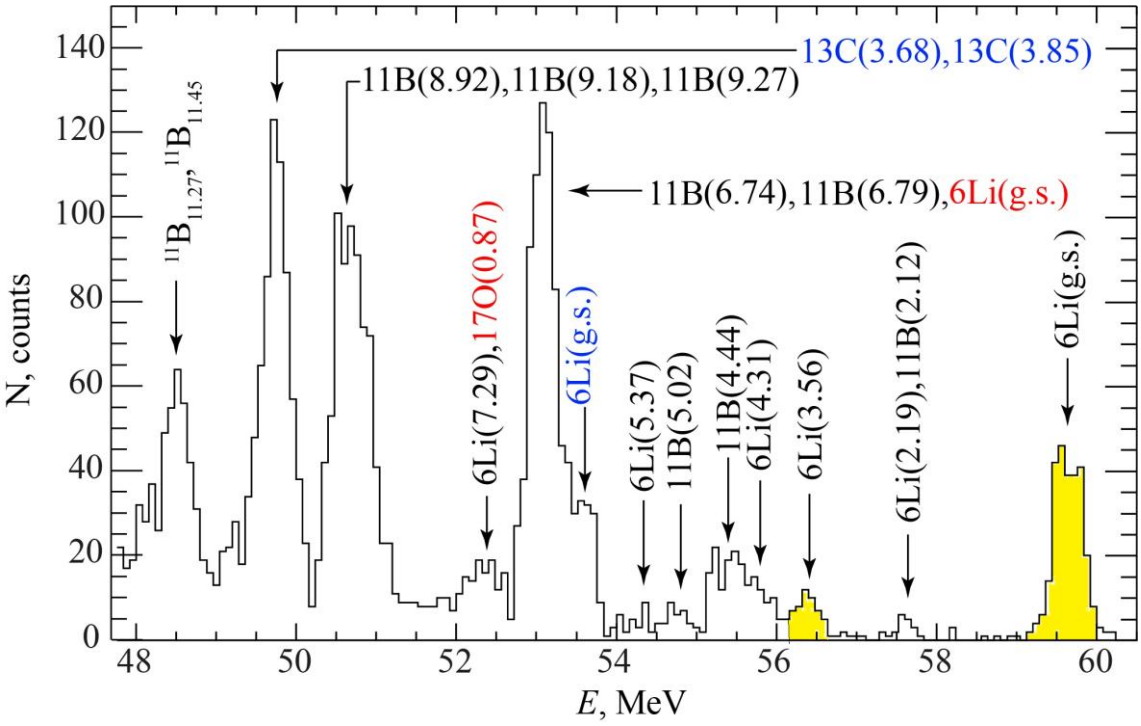

Fig. 8: Energy ($\Delta E + E$) spectrum of ^{6}Li recorded at $\theta_{LAB} = 10^{o}$. Black color indicates the ^{6}Li peaks from the reaction on the ^{10}B target, blue and red indicate the ^{6}Li peaks obtained in reactions on ^{12}C and ^{16}O impurities, respectively.

3.2 Differential cross section extraction method

The differential cross section of the reaction is determined based on the relationship between the yield, the target nucleus density, the incident beam intensity, and the solid angle of the detector, according to the following expression (1):

$$\frac{d\sigma}{d\Omega} = \frac{Y}{N_p \times N_t \times \Delta\Omega} \quad (1)$$

Y is the reaction yield; **Np** and **Nt** are the number of incident ^{7}Li (dependent on the beam intensity **I**) and the number of target nuclei (dependent

on the target thickness), respectively; $\Delta\Omega$ is the solid angle of the detector; and $\frac{d\sigma}{d\Omega}$ is the differential cross section of the reaction.

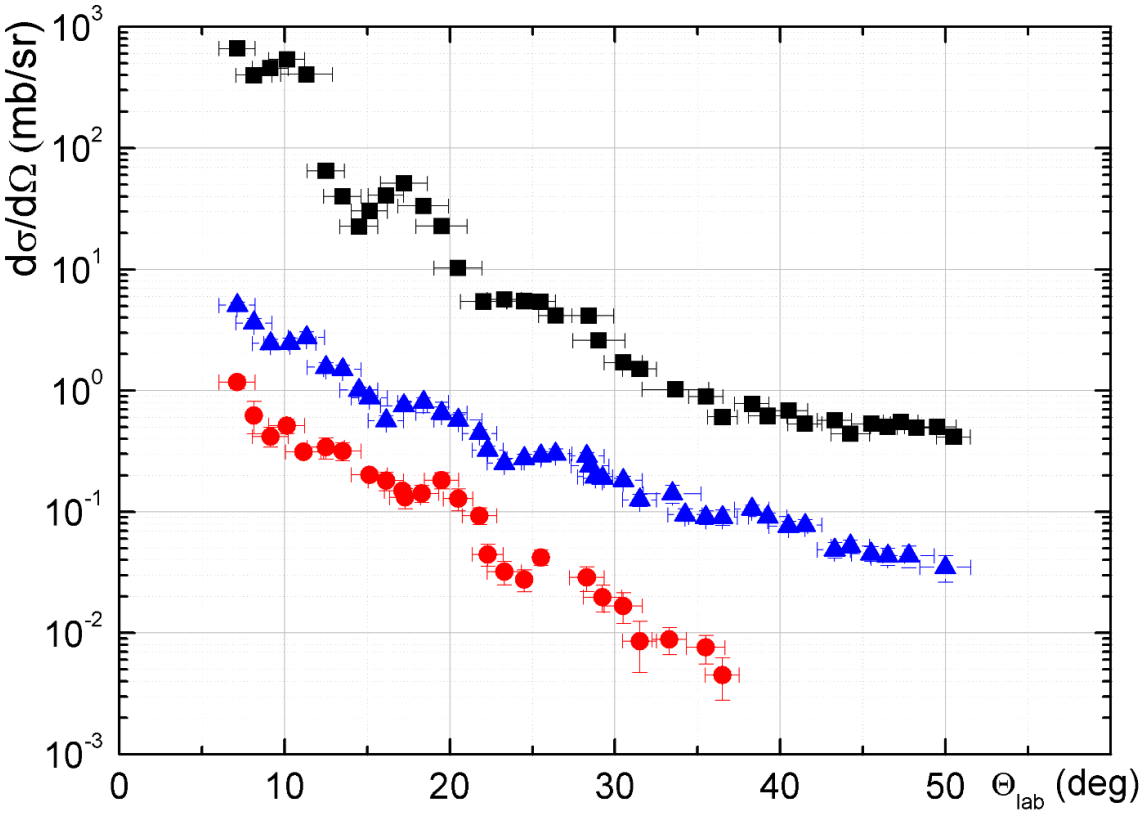

Fig.9 : Angular distributions of differential cross sections of elastic scattering of (^{7}Li+^{10}B) and reaction channels of transfer ^{10}B(^{7}Li,^{6}Li)^{11}B to the ground ^{6}Li and excited ^{6}Li($J^{\pi} = 0^{+}$, $T = 1$, E = 3.56 MeV) states of ^{6}Li. Black squares correspond to elastic scattering of ^{7}Li+^{10}B blue triangles to the ground state of ^{6}Li$_{g.s.}$, red circles to the excited state of ^{6}Li($J^{\pi} = 0^{+}$, $T = 1$, E = 3.56 MeV).

Fig. 10 below presents the angular differential cross section of the reaction ^{10}B(^{7}Li,^{7}Be$_{g.s}$)^{10}Be , measured in the laboratory frame over an angular range from 15° to 45°. The resulting angular distribution clearly exhibits the characteristic behavior of a charge exchange reaction, with the differential cross section decreasing rapidly as the laboratory angle increases, reflecting the dominance of forward scattering. This spectral shape is a typical signature of direct reaction mechanisms, where the overlap between the initial and final nuclear wave functions plays a decisive role in determining the reaction probability. The slope of the angular spectrum not only reflects the dynamics of

nucleon transfer but also provides quantitative insight into the nuclear structure of the participating systems, particularly the matter density distribution and the role of cluster components within ^{7}Li and ^{10}B. Precise analysis of the differential cross section at various angles enables validation of theoretical models such as DWBA, allowing extraction of form factors and transition wave functions. These data not only clarify the microscopic nature of the proton transfer process but also contribute to a deeper understanding of spin-isospin structure and reaction dynamics in light nuclear systems near stability.

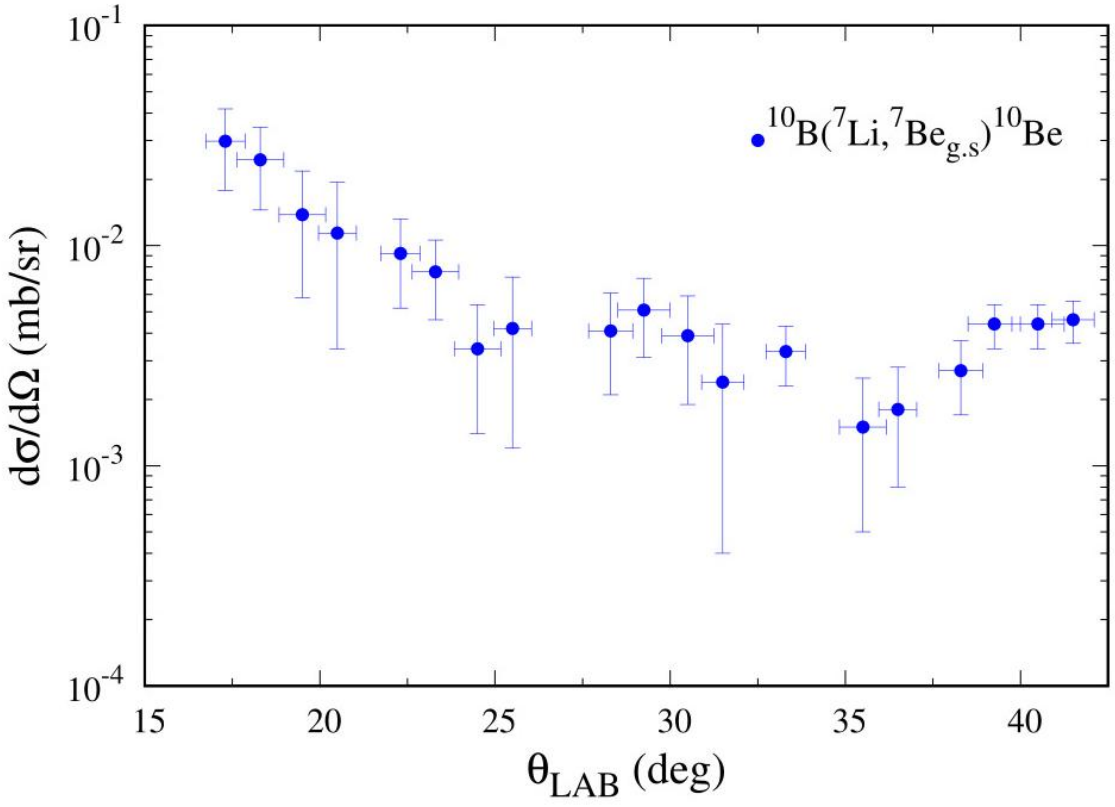

Fig. 10: Angular distribution of differential cross sections for the reaction ^{10}B(^{7}Li,^{7}Be$_{g.s.}$)^{10}Be.

IV. Conclusion

1. During "Start" project, I studied the motivation and goals of the experiment for measuring the differential cross sections of the ^{7}Li+^{10}B reaction products. The key points of the experiment are outlined in the Introduction section.

2. To complete the project's objectives, I learned the particle identification method based on ionization energy loss in a dE-E telescope of silicon detectors. I performed calculations of the energy loss for ^{3,4,5}He, ^{6,7,8}Li, and ^{7,9,10}Be particles in the dE (30μm) and E (700μm) Si detector layers using the LISE^{++} framework. These calculations formed the basis for identifying the charged particles.

3. As a training exercise in experimental data analysis, an angular analysis of the 6Li reaction product yields was conducted under the supervision of the research group. The angular dependences of the ^{6}Li*g.s.* differential cross sections were plotted and found to be in agreement with published data [11], presented in Figure 9.

4. Following training in the analysis methodologies, the team performed an analysis of the angular dependences for the ^{7}Be*g.s.* differential cross sections. The resulting data from this analysis will be used in the future for theoretical studies of charge exchange reactions.

References

1. I. Tanihata *et al.,* Phys. Rev. Lett. **55,** 2676, (1985);
2. A.V. Dobrovolsky, *et al.*, Nucl. Phys. **A 766**, pp..1–24, (2006);
3. D.M. Rodkin, Yu.M. Tchuvil'sky, "Sizes of the Neutron–Proton Halo in Nucleon-Stable States of the ^{6}Li Nucleus", JETP Lett., **118**(3), 153, (2023);
4. Bull. RAS 72 (3), p.356, (2008);
5. Sobolev Yu. G., Budzanowski A., Bialkowski E., *et al.,* Bull. RAS **69** (11), p.1605, (2005);
6. http://cdfe.sinp.msu.ru/services/radchart/radmain.html.
7. Arai K, Suzuki Y and Varga K. Phys Rev **C 51**, 2488, (1995);
8. Arai K. *et al*, Phys Rev **C 54,** 132, (1996);
9. Jelavic Malenica D., Milin M., Di Pietro A., *et al.*, Phys Rev **C 112**, 044302, (2025);
10. Tarasov O. B., Bazin D. NIM **B 266**, 4657-4664. (2008);
11. S.S. Stukalov, Yu.G.Sobolev, Yu.E.Penionzhkevich *et al.,* Physics of Atomic Nuclei **87**, 426 (2025).